Construction and Building Materials 109 (2016) 8–16

Contents lists available at ScienceDirect

Construction and Building Materials

journal homepage: www.elsevier.com/locate/conbuildmat

Comparative evaluation of fatigue resistance of warm fine aggregate asphalt mixtures

Mohammed Sadeq [a,b,*], Hussain Al-Khalid [a], Eyad Masad [b], Okan Sirin [c]

[a] Centre for Engineering Sustainability, School of Engineering, University of Liverpool, Liverpool, UK
[b] Mechanical Engineering Program, Texas A&M University at Qatar, Doha, Qatar
[c] Department of Civil & Architectural Engineering, College of Engineering, Qatar University, Doha, Qatar

HIGHLIGHTS

- Using WMA additives increased the stiffness of the asphalt mixture.
- Sasobit mix has dissipated less energy with cycles than other mixes.
- VECD method showed insignificant difference between HMA and WMA in fatigue resistance.
- FAM samples showed less variability among replicates than AMPT-sized samples.

ARTICLE INFO

Article history:
Received 18 September 2015
Received in revised form 21 January 2016
Accepted 26 January 2016

Keywords:
WMA
FAM
Fatigue
VECD
DPSE
Sasobit
Advera
Rediset

ABSTRACT

Fatigue cracking is one of the crucial distresses in asphalt pavements that affect its service life and rehabilitation process. The resistance of asphalt mixtures to fatigue failure in the laboratory experiments is influenced by several factors such as temperature, loading frequency, loading mode, sample type and geometry. This study focused on the evaluation of fatigue performance of different types of warm mix asphalt (WMA) mixture and comparing them with a hot asphalt mixture (control mixture). Warm fine aggregate mixtures (W-FAM) were fabricated using three different WMA additives: Advera, Sasobit, and Rediset which were short-term aged in the laboratory. Then, the W-FAM specimens were exposed to shear stress oscillation test by applying damaging stress level in the dynamic mechanical analyser (DMA) to examine the material fatigue resistance. The test results were analysed using the viscoelastic continuum damage (VECD) approach. The W-FAM exhibited lower dissipated pseudo-strain energy (DPSE) than the control mixture. However, there was no statistical significant difference between the W-FAM and control mix in terms of the number of cycles to failure resulted from the VECD analysis.

1. Introduction

Fatigue cracking is one of the main distresses in the asphalt pavements that affect its service life. Studying fatigue performance attracted the attention of many researchers since 1858 due to its complexity and importance in rehabilitation or replacement decision of the entire pavement [1–3]. More robust understanding of factors that affect fatigue cracking would advance the design of long lasting pavements.

The resistance of asphalt mixtures to fatigue failure in laboratory experiments is affected by various factors: temperature, loading frequency, loading mode, sample type and geometry. Evaluation of fatigue resistance can be performed using Asphalt Mixture Performance Tester (AMPT) apparatus on full mixture field-cut or lab-fabricated specimens. However, the heterogeneity of full asphalt mixture specimens causes high variability in fatigue testing results, which makes it difficult to predict field performance with reasonable reliability [4,5]. An alternative is to test fine aggregate mixture (FAM) specimens, which contain the fine portion of the mixture. FAM specimens have higher uniformity and yield less variability in fatigue testing results than full mixture-sized samples [6].

Several analytical approaches have been used to determine fatigue performance; however, the viscoelastic continuum damage

* Corresponding author at: Mechanical Engineering Program, Texas A&M University at Qatar, Doha, Qatar.

E-mail addresses: mohammed.sadeq@liverpool.ac.uk, mohammed.sadeq@qatar.tamu.edu (M. Sadeq), khalid@liverpool.ac.uk (H. Al-Khalid), eyad.masad@qatar.tamu.edu (E. Masad), okansirin@qu.edu.qa (O. Sirin).

http://dx.doi.org/10.1016/j.conbuildmat.2016.01.045
0950-0618/

(VECD) approach that implements Schapery's theory is the most developed and used [7]. The main principle of VECD is calculating the dissipated pseudo-strain energy (DPSE), which is based on the concept of separating the dissipated energy due to damage from energy dissipated because of viscoelastic behaviour. Masad et al. used that concept and identified three main components for DPSE that are associated with change in phase angle between load cycles; change in phase angle within single cycle; and change in stiffness between cycles [8]. Masad et al. showed that the VECD approach can unify the predictions from the strain and stress controlled loading modes.

The fatigue performance of warm mix asphalt (WMA) is of interest because of the significant increase in using WMA additives given their environmental and energy-saving advantages. For example, Zelelew et al. used the fatigue factor ($|E^*|\cdot\sin\delta$) which combines the dynamic modulus ($|E^*|$) and the phase angle (δ) [9] to study fatigue resistance of WMA. The study concluded that using WMA additives reduced the fatigue cracking resistance for asphalt mixtures. Kim et al. used the Dynamic Shear Rheometer (DSR) to test asphalt binders mixed with two WMA additives: Aspha-min and Sasobit [10]. The study compared the shear complex fatigue factor ($|G^*|\cdot\sin\delta$) and also concluded that WMA additives reduced the fatigue resistance of the asphalt binders. Haggag et al. tested long-term aged WMA mixtures by the uniaxial cyclic direct tension–compression test [11]. The experimental results were analysed by the VECD analysis approach to evaluate the fatigue performance. The results showed that there was no significant difference between hot mix asphalt (HMA) and WMA samples in fatigue cracking resistance except for the WMA prepared using Advera additive. Safaei et al. also tested long-term aged WMA and HMA and showed that HMA has better fatigue performance compared with WMA mixtures [12].

2. Objectives

The main purpose of this work is to evaluate the fatigue cracking resistance of short-term aged warm fine aggregate mixtures (W-FAM) modified with different WMA additives. Shear stress oscillation test was performed on control FAM without WMA additive and W-FAM modified with three additives (Advera, Sasobit, and Rediset). The test results were analysed using the VECD approach to determine the number of cycles to fatigue failure.

3. Sampling and testing scheme

In order to study the influence of WMA additives on fatigue resistance of asphalt mixtures, a testing scheme was developed by fabricating fine aggregate mixture (FAM) samples in the laboratory. Samples were prepared using "Gabbro" aggregate and polymer modified PG 76-22 asphalt binder. Gabbro aggregate is imported to the State of Qatar from the United Arab Emirates. The bitumen was originally imported from the Kingdom of Bahrain and locally modified with SBS polymers to produce PG76-22 grade. The modified asphalt binder was mixed with three WMA additives: Sasobit, Advera, and Rediset using high shear mixer at dosages of 2%, 5%, and 0.5% of binder's weight, respectively.

Sasobit, is an organic (wax) WMA additive produced from natural gas using the Fisher Tropsch process of polymerisation by Sasol Wax in South Africa. It has the potential to increase the stiffness of asphalt binder and reduce its viscosity in order to help mixing and compaction at lower temperatures [13]. Advera is a water-based additive that releases water particles while mixing with binders to lower its viscosity by foaming mechanism [14]. On the other hand, Rediset LQ is a chemical liquid additive that has no influence on the mechanical properties of asphalt binder; however, it lessens the viscosity to allow lower mixing and compaction temperatures [15].

Dynamic Shear Rheometer (DSR), shown in Fig. 1(a), from Malvern (Kinexus Pro model), was used to perform the fatigue testing. The instrument was provided with a special fixation for finger samples end connections as shown in Fig. 1(b). The upper fixation rotates while the lower is fixed. The maximum shear force the machine can reach is 600 kPa. In addition, the machine was provided with a temperature chamber (Fig. 1(a)) that keeps the temperature uniform at 25 °C during the test.

The aggregate gradation for the FAM design is based on the proportional ratio of Job Mix Formula (JMF) from the full HMA gradation. Table 1 shows the original mix design and FAM gradation [16,17]. FAM gradation was calculated starting from 1.18 (N16) sieve size by dividing the retained value of all sieves from 0.6 (N30) sieve by the passing percentage of 1.18 (N16) sieve size. The mixture was prepared in the laboratory to achieve the required sample height of 110 mm after compaction and provide enough height for cutting it for testing at 50 mm height.

Asphalt binder content was estimated for the FAM design by burning the binder content from a prepared and separated loose HMA sample using the ignition oven. Loose HMA mix was separated by hand and then sieved to obtain the portion of the mix with particles passing sieve 1.18 mm (N16). This fine mix was placed in the ignition oven to burn the binder and determine its weight. The results showed that the binder content of fine mix part was 7.3% of the total mix weight. Two samples of 150 mm diameter were prepared for each additive type. Table 2 shows the mixing and compaction temperatures for different additives used in this study.

Mixing and compacting asphalt mixtures at lower temperatures reduces the ageing that could occur in the material due to heating. The WMA mixtures were mixed at 145 °C based on common practice and previous knowledge with polymer modified binders with WMA additives. The specimens were compacted at 116 °C following the recommendations of the NCHRP 763 report and it also meets the typical criteria of compacting the WMA samples at least 15 °C below of the HMA compaction temperature [18,19].

A total of six cylindrical specimens were extracted from the compacted samples by coring and cutting them to 12 mm diameter and 50 mm height. A drilling machine (Cardi brand) was used with 12 mm inner diameter coring bit to extract the specimens from each mixture sample. On average, the percentage of air voids was about 3% in the cylindrical samples.

4. Experimental work

4.1. Stress sweep test

Categorising the linear and nonlinear viscoelastic properties of tested materials was done by performing stress sweep test [20]. The test was started from a stress value of 1 kPa and increased by 25 kPa every 20 s until it reached 589 kPa before termination.

Experimental data were analysed by calculating the strain slope at each stress level and plotting it against stress level as shown in Fig. 2. The figure indicates that any oscillation stress level before 150 kPa can be considered to be in the linear viscoelastic region of the materials, while any stress level above 150 kPa oscillation stress might expose the material to nonlinearity and then damage. This test was performed at 25 °C temperature and 10 Hz frequency.

4.2. Relaxation test

Relaxation test, which involves applying constant strain for a certain period of time, was performed to measure the relaxation modulus of the material. The strain amplitude value used was

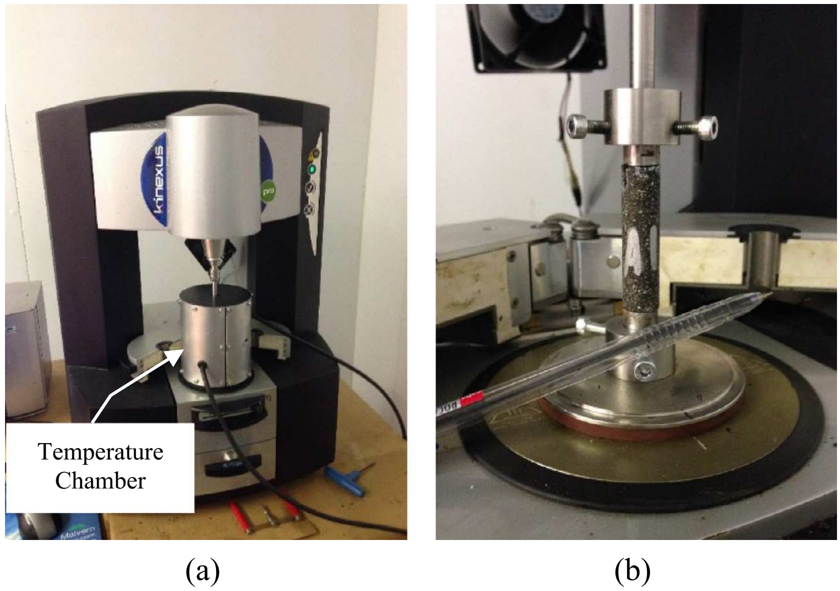

Fig. 1. (a) DSR used for fatigue testing with the temperature chamber. (b) Cylindrical samples after fixed to upper and lower fixations.

Table 1
Aggregate gradation for Original mix design and fine aggregate mix design.

Sieve size, mm (in)	Control mix design		FAM mix design	
	% Passing	Retain %	% Passing	Retain %
37.5 (1 1/2″)	100.0%	0	–	–
25 (1″)	98.6%	1.4%	–	–
19 (3/4″)	88.2%	10.4%	–	–
12.5 (1/2″)	76.9%	11.3%	–	–
9.5 (3/8″)	68.9%	8.0%	––	–
4.75 (N4)	47.1%	21.8%	–	–
2.36 (N8)	26.5%	20.6%	–	–
1.18 (N16)	15.8%	10.7%	100%	0.0%
0.6 (N30)	10.5%	5.3%	66.5%	33.5%
0.3 (N50)	7.9%	2.6%	50.0%	16.5%
0.15 (N100)	6.1%	1.8%	38.6%	11.4%
0.075 (N200)	4.2%	1.9%	26.6%	12.0%
Pan	0.0%	4.2%	0.0%	26.6%
Total		100.00%		100.00%

Table 2
Mixing and compaction temperatures for HMA and WMA.

	Original	Sasobit	Advera	Rediset
Mixing, °C	163	145	145	145
Compaction, °C	135	116	116	116

0.005% and was within the linear viscoelastic region associated with the linear stress level specified by the stress sweep test.

Experimental data of instantaneous relaxation modulus are plotted against time in Fig. 3, which shows typical relaxation test experimental data and fitted curve used to estimate the relaxation test parameters G_1^*, G_1^* and m of Eq. (1):

$$G^*_{relaxation} = G_1^* + G_1^* \times t^{-m} \quad (1)$$

where G_1^* represents the shear modulus that the material would reach at infinite time. However, for all tested materials, G_1^* was optimised to zero. G_1^* represents the starting shear modulus at the beginning of relaxation and 'm' value presents the slope of relaxation curve [21]. Higher 'm' value indicates a more rapid drop of G_1^* that initiate a quick reduction in shear modulus.

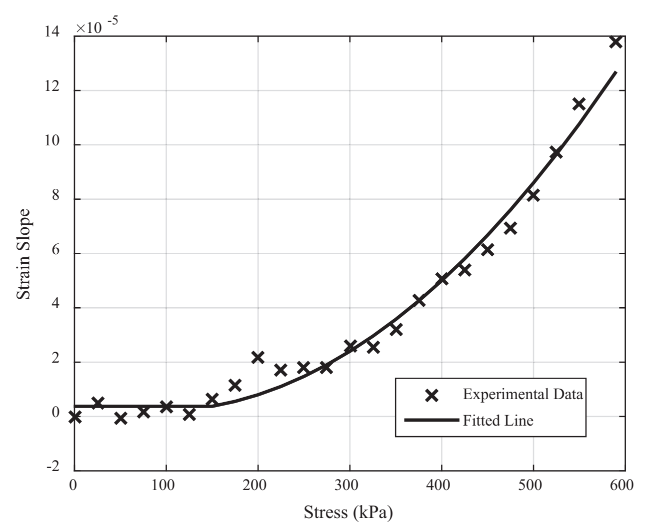

Fig. 2. Stress sweep test analysis for defining linear and nonlinear region in material response.

4.3. Fatigue test

Two stress amplitudes were applied to the samples, low-stress (75 kPa) that is within the linear viscoelastic response and high-stress (400 kPa) that causes damage to the specimens. The low-stress level test is applied at 10 Hz for 2 min followed by the high-stress level test that was terminated after 200,000 cycles even if a complete failure does not occur. The failure criterion was chosen to be when the specimen reaches 50% of its starting shear modulus [22].

5. Analysis methods & results

Testing cylindrical samples at low stress level was performed in order to determine relaxation modulus, dynamic modulus and phase angle within the linear viscoelastic range. In addition, tests were performed at damaging stress level to determine dynamic

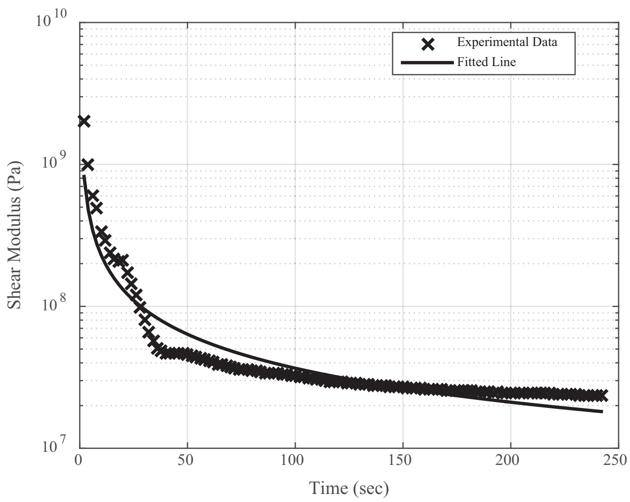

Fig. 3. Typical relaxation test data results and fitted curve.

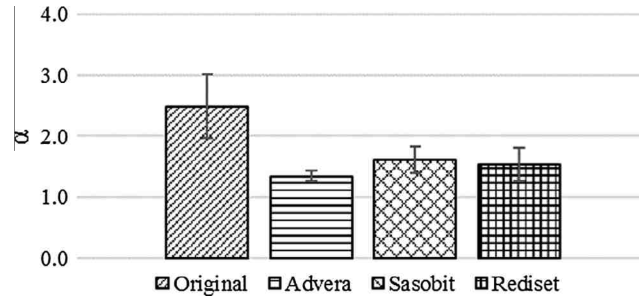

Fig. 4. Averaged 'α' values for the original (control mix) and WMA mixes.

modulus and phase angle within the nonlinear viscoelastic range and fatigue damage.

5.1. Relaxation test

The instantaneous shear modulus values from the relaxation test experimental data were plotted in logarithmic scale and fitted with power law relationship stated in Eq. (1). As mentioned earlier, G_1^* values for all mixes are zero while average values of 'G_1^*' and 'm' are listed for all mixes in Table 3.

The value of 'm' is then used to calculate the constant value of '$\alpha = 1/m$' that will be used later in the VECD analysis method [23]. As shown in Fig. 4, average 'α' value was plotted with the standard error bars for each mix type and shows some variability among replicates. This variability would have a considerable effect on pseudo-stiffness calculation. The average value of 'α' was used for each mix to emphasise the variability between replicates.

5.2. Fatigue test at low-stress level

Stress oscillation test was conducted after the relaxation test to obtain the dynamic linear viscoelastic properties of each mix. The experimental data were averaged to determine single shear modulus ($|G^*|$) and phase angle (δ) values.

Fig. 5 shows results from low-stress oscillation test demonstrating that the addition of Sasobit to asphalt mixtures increased the shear modulus ($|G^*|$) and decreased the phase angle (δ). It is also noticeable that Rediset had only a minor influence on the stiffness of the material while the average shear modulus is close to the original mixture. It is also obvious from Fig. 5(c) that all WMA mixes have higher fatigue factor than control mix.

5.3. Fatigue test at high-stress level

Fatigue test at high-stress level was conducted on the same samples after the low-stress level test. The instrument was set to apply oscillation shear stress of 400 kPa stress level and 10 Hz frequency. The software was configured to capture the shear modulus and the phase angle during loading cycles as shown in Fig. 6. Typically, the shear modulus passes through three stages during fatigue testing: rapid reduction within small number of cycles; steady and slow reduction for many cycles; and finally very rapid reduction leading to failure [24]. However, in this study, shear modulus did not reach total failure or break before the end of the test.

5.4. Dissipated pseudo-strain energy (DPSE) method

For viscoelastic materials, part of the energy applied during loading dissipates and does not recover upon unloading [24–26]. However, viscoelastic materials dissipate even more energy if they are damaged during loading. The dissipated energy associated with damage can be determined by calculating the dissipated pseudo strain energy (DPSE). Masad et al. proposed that the DPSE can be separated into three components [27]. The first component (W_{R1}) is associated with an increase in apparent phase angle and is calculated as follows:

$$W_{R1} = \pi \frac{\tau_{0F}^2}{G_{LVE}^*} \sin(\delta_{NF} - \delta_{LVE}) \quad (2)$$

where τ_{0F} is the stress amplitude (Pa) applied to the specimen during the test. G^*_{LVE} and δ_{LVE} are the linear viscoelastic shear modulus and phase angle obtained from the low-stress level test. Then δ_{NF} is the phase angle at each cycle. The second component of DPSE method is (W_{R2}) which is associated with the change in phase angle within each cycle. In this study, the phase angle for each cycle is averaged within the stress–strain wave. Hence, this component has been ignored in the analysis presented herein [28]. The third component of DPSE (W_{R3}) is for the difference between pseudo-stiffness for undamaged material and pseudo-stiffness after damage. This component can be calculated using Eq. (3) as follows:

$$W_{R3} = \frac{1}{2} \tau_{0F}^2 \left(\frac{1}{G_{NF}^*} - \frac{1}{G_{LVE}^*} \right). \quad (3)$$

where G^*_{NF} is the shear modulus at each cycle. Finally, W_{R1} and W_{R3} were summed and plotted against the number of cycles (N). Higher W_R ($W_{R1} + W_{R2}$) indicates that the material dissipate more energy during the damage process. A Matlab code (version R2012a) was developed to perform all calculations for this analysis method.

Table 3
Values of 'G_1' and 'm' from relaxation test for each mix.

	Original		Advera		Sasobit		Rediset	
	G_1^*	m	G_1^*	m	G_1^*	m	G_1^*	m
Average	7.30×10^8	0.532	1.58×10^9	0.757	3.69×10^9	0.718	1.83×10^9	0.769
Standard Deviation	5.89×10^8	0.330	4.98×10^8	0.103	4.40×10^9	0.223	2.02×10^9	0.263

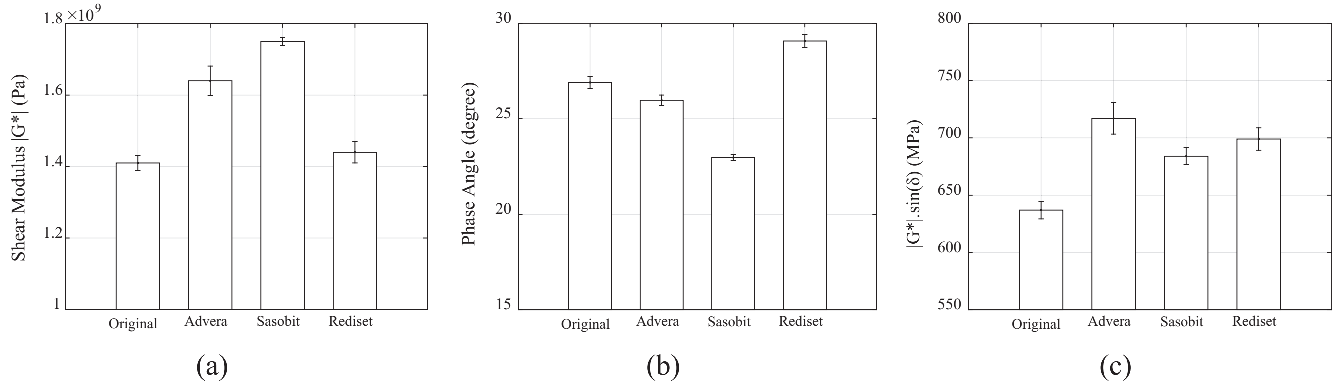

Fig. 5. Average values of (a) complex modulus, (b) phase angle, and (c) fatigue factor for each mix.

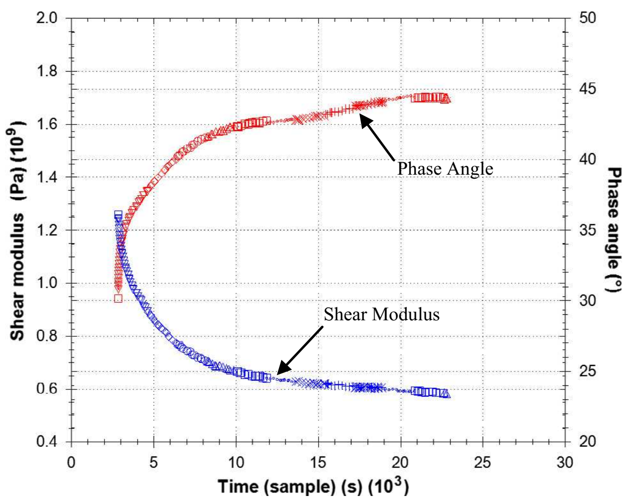

Fig. 6. Typical raw experimental data obtained from instrument software for high-stress fatigue test.

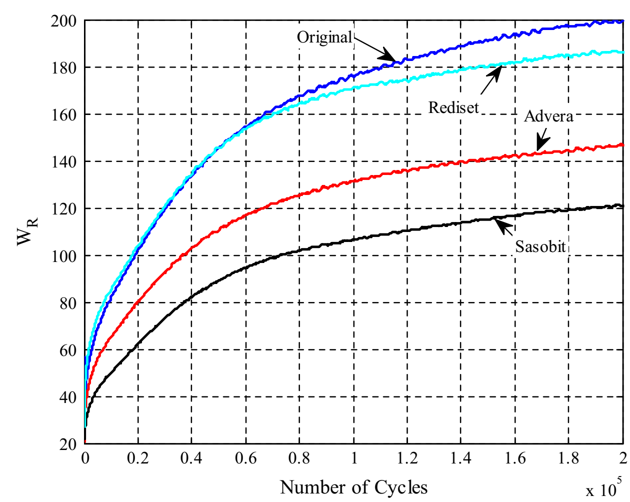

Fig. 7. Results of DPSE method (W_R) for each mix.

Results from the DPSE method shown in Fig. 7(a) revealed a similar conclusion to linear viscoelastic behaviour. Rediset has a minor influence on the asphalt mixtures and almost matching the original mixture particularly at early life. Sasobit presented lowest dissipated energy with number of cycles among all mixes. Results indicate that asphalt mixtures mixed with Sasobit would dissipate less energy to reach 200,000 cycles while other materials would dissipate more to reach the same number of cycles.

Similarly, by plotting the hysteresis loops after 200,000 cycles for all mixes as shown in Fig. 8, it is observable that Sasobit has the smallest area inside the hysteresis loop, and the original mix has the largest. These loops are generated using the experimental data at a specific cycle.

However, the DPSE alone does not give full assessment of the resistance to fatigue damage. The viscoelastic continuum damage (VECD), which incorporates DPSE along with other material properties is used in this study to quantify the fatigue damage.

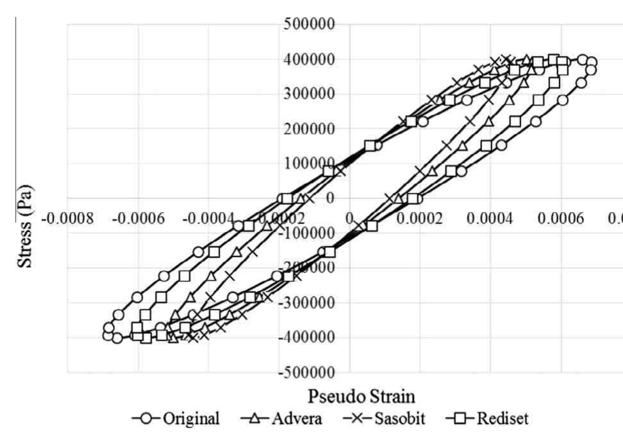

Fig. 8. Hysteresis loop after 200,000 cycles for Original, Advera, Sasobit, and Rediset mixtures.

5.5. Viscoelastic continuum damage (VECD) Approach

Researchers used various aspects of VECD to analyse fatigue performance of asphalt mixtures by estimating the number of cycles to failure. The VECD approach is based on Schapery's elastic–viscoelastic principle that quantify damage growth inside a specimen [6,28]. Analysing the fatigue behaviour using this theory is based on calculating pseudo-strain 'ε^R', pseudo-stiffness '*C*', and internal damage parameter '*S*'. Reduction in material properties due to damage is presented by the pseudo-stiffness '*C*' parameter. Psuedo-stiffness can be calculated by dividing shear modulus (G^*_N) at each cycle by linear viscoelastic shear modulus (G^*_{LVE}), as shown in Eq. (4):

$$C_N = \frac{G^*_N}{G^*_{LVE}} \quad (4)$$

Damage parameter '*S*' presents the damage growth in the material and can be calculated for stress-controlled test as follows [23]:

$$S_{N+\Delta N} = S_N + \left(\frac{\Delta N}{f}\right)^{\frac{1}{1+\alpha}} \left[\frac{0.5}{I}\sigma_N^{R^2}\left(\frac{1}{C_{N+\Delta N}} - \frac{1}{C_N}\right)\right]^{\frac{\alpha}{1+\alpha}} \tag{5}$$

where S_N is the internal damage at each cycle starting from the initial damage (S_0), ΔN is the difference between number of cycles which fixed in this study to be 2000 cycles. 'f' is the frequency and 'α' is a constant related to the rate of damage growth and depends on failure zone characterisation [29,30]. As mentioned earlier, 'α' is considered to be $(1/m)$ where 'm' is the maximum slope obtained from the relaxation test. Finally, σ_N^R is the peak pseudo-stress calculated by dividing the peak stress at each cycle by the linear viscoelastic shear modulus as shown in Eq. (6). The value of 'I' in this case is the ratio of first shear modulus value at the beginning of the test and the linear viscoelastic shear modulus. This assumption was made to eliminate sample to sample variability [23].

$$\sigma_N^R = \frac{\sigma_N}{G^*_{LVE}} \tag{6}$$

Kutay et al. defined the damage for micro cracks by eliminating the effect of unstable applied stress or strain in the damage analysis [31]. In order to accommodate that, C–S curves presented in Fig. 9 are simulated using the material behaviour parameters ('a' and 'b') which are then used with the true stress value to calculate the true C–S curves. The exponential Eq. (7) was used to obtain the constant parameters ('a' and 'b') and fit the experimental data to simulate C–S curves with the true pseudo-stress value.

$$C_N = \exp(aS_N^b). \tag{7}$$

Values of 'a' and 'b' obtained by fitting the experimental data are presented in Fig. 10. The figure shows the standard error, which is calculated by dividing the standard deviation over the square root of sample size. It can be noticed that the variability in values of 'a' is much higher than in values of 'b'. The variability may affect the calculation of simulated pseudo-stiffness that are based on modelling experimental data behaviour.

The simulated damage parameters '$S_{Simulated}$' was calculated then by Eq. (8) for stress-controlled test and plotted against simulated pseudo-stiffness '$C_{Simulated}$' which is calculated by Eq. (9):

$$S_{Simulated}^{N+\Delta N} = S_N + \left(\frac{\Delta N}{f}\right)\left[\frac{0.5}{I}\sigma_N^{R^2}\frac{dC^{-1}}{dS}\right]^{\alpha} \tag{8}$$

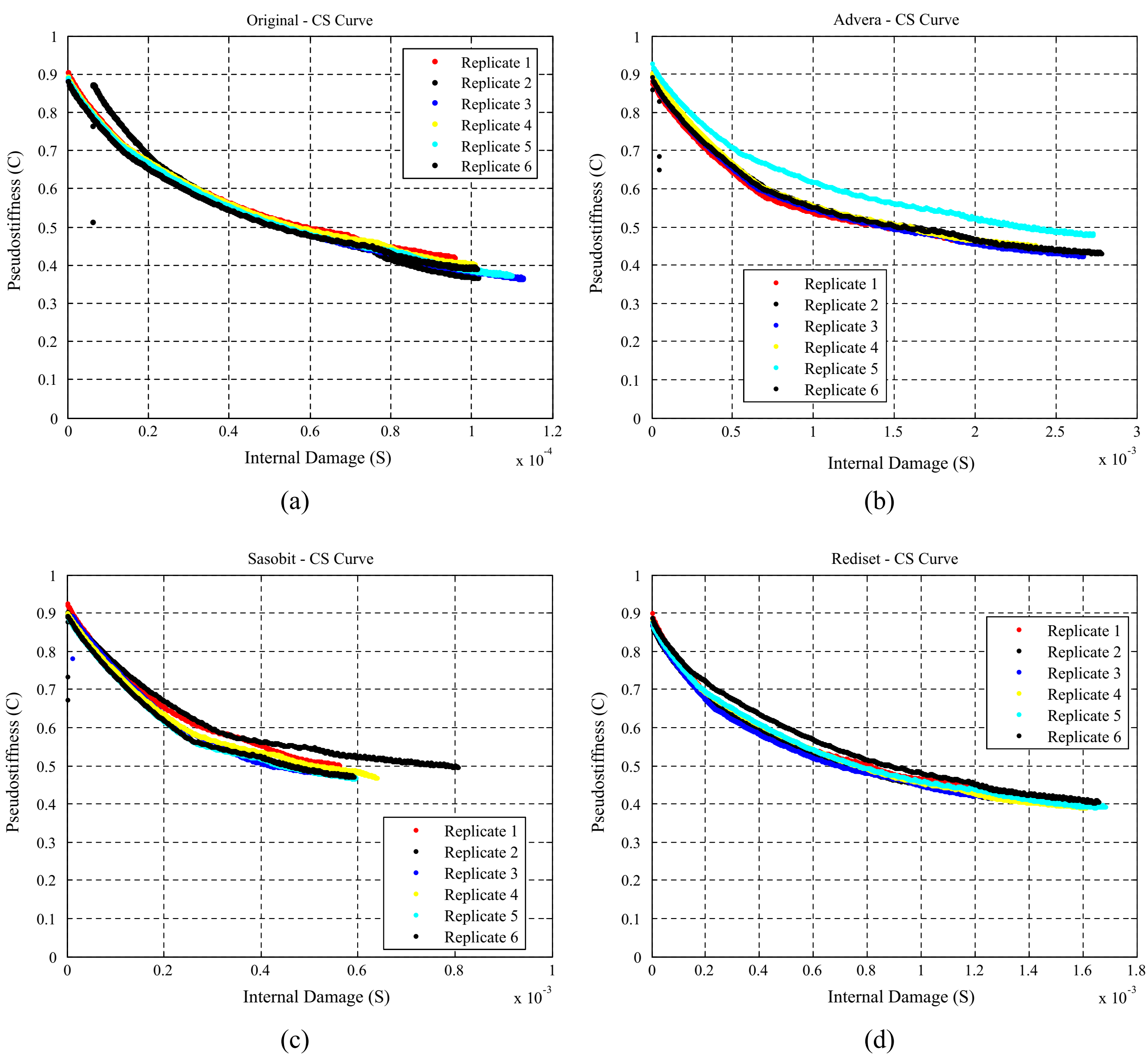

Fig. 9. Experimental C–S curves for all replicates of (a) Original (control) mix, (b) mix with Advera, (c) mix with Sasobit, (d) mix with Rediset.

Fig. 10. Average of (a) '*a*', (b) '*b*' values for each mix.

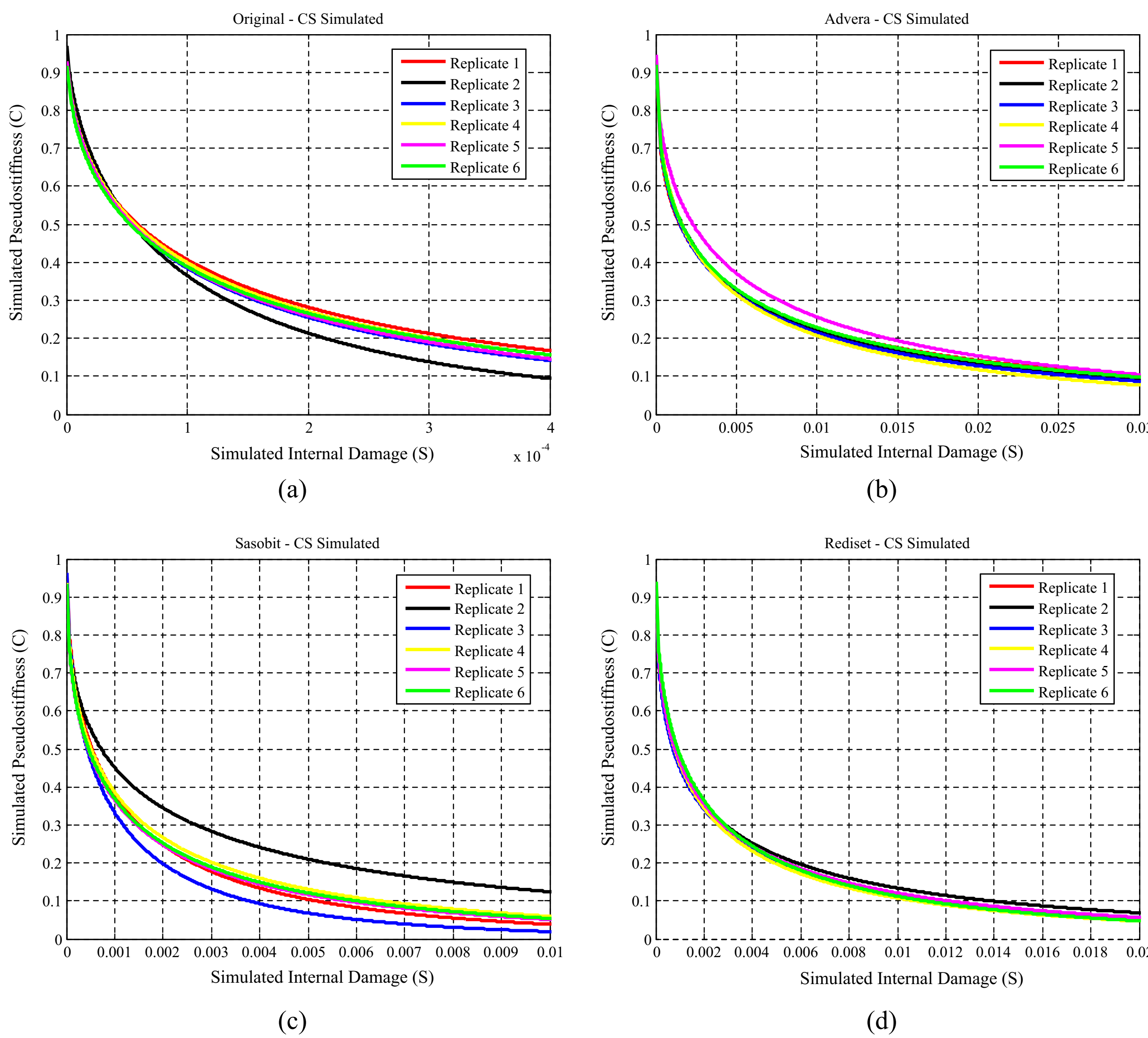

Fig. 11. Simulated *C*–*S* curves for all replicates of (a) Original mix, (b) mix with Advera, (c) mix with Sasobit, (d) mix with Rediset.

$$C_{Simulated} = \exp(aS^b_{Simulated}). \quad (9)$$

Since the machine could not keep the stress amplitude absolutely constant during the whole test, σ^R_N is calculated using the true pseudo-stress (Eq. (10)). By using this technique, creating simulation analysis of the material behaviour gives the ability to use any stress amplitude and consequently simulate the material performance. In this analysis, the true stress (σ_{true}) is considered as 400 kPa for the destructive test based on stress sweep analysis results.

$$\sigma^R_N = \frac{\sigma_{true}}{G^*_{LVE}}. \quad (10)$$

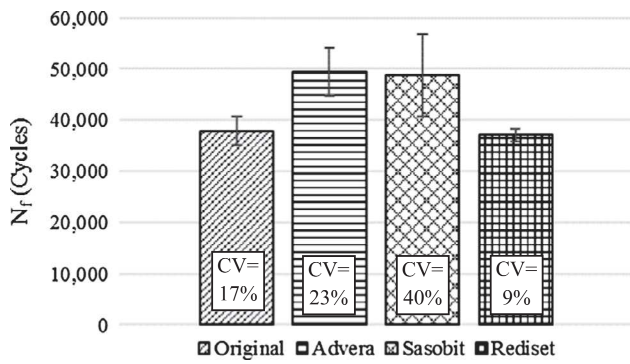

Fig. 12. Number of cycles to 0.5 simulated pseudo-stiffness failure for each mix.

The term $\frac{dC^{-1}}{dS}$ in Eq. (8) is computed by partial derivative of Eq. (7) to be:

$$\frac{dC^{-1}}{dS} = -\left(e^{-aS^b}\right)abS^{b-1} \quad (11)$$

Eq. (7) is then converted to measure the number of cycles to failure 'N_f' by identifying the level of pseudo-stiffness reduction failure criteria 'S_f' as in Eq. (12):

$$S_f = \left(\frac{\ln C_f}{a}\right)^{1/b} \quad (12)$$

Failure in fatigue test can be identified based on several criteria, such as (a) complete break of sample, (b) reaching maximum phase angle, (c) drop of 50% in sample stiffness or 90% in sample complex shear modulus [21,31–33]. In this study, C_f in all cases was assigned to 0.5 to calculate the damage parameter (S_f) at 50% reduction in stiffness. Finally, N_f was calculated by integration from S_0 to S_f while S_0 represents the assumed initial internal damage in the material as in Eq. (13):

$$N_f = \int_{S_0}^{S_f} \left[\frac{\sigma_N^{R^2}}{2I}\frac{dC^{-1}}{dS}\right]^{-\alpha} fdS \quad (13)$$

Obtaining 'N_f' requires an assumption to be made for the initial damage (S_0) for the mix and each replicate. The analysis is very sensitive to the initial damage (S_0) value. In this study, we have used the approach recommended by Underwood et al. [34] to select S_0 such that there is minimal damage at the beginning of the test and smooth reduction in pseudo-stiffness with cycles. In this study, each replicate of a mix had a unique initial damage value. However, all of initial damage values were chosen to be lower than 0.0001. The choice of low values was to ensure minimal initial damage since these samples are lab-fabricated samples and did not suffer from damage yet. Based on all factors mentioned above, Fig. 11 shows six replicates of simulated C–S curves for each mixture.

As shown in Fig. 11, replicates are smoother after simulating the experimental data. However, Sasobit has more scatter than other mixes. This scatter is mostly due to the initial damage assigned for the replicate in the simulation part of the analysis.

By calculating the number of cycles to failure (N_f) for each mixture using Eq. (13), average results plotted in Fig. 12 show that Sasobit and Advera mixes have higher variability than other mixes. The Coefficient of Variance (CV) for Sasobit mix is 40%; however, it is still lower than the AMPT-sized results reviewed in the literature with similar material [5]. All mixes showed short fatigue life with number of cycles to failure between 30,000 and 50,000 cycles. This indicates that the fatigue test performed at 400 kPa was high enough to damage the samples at early life.

It can also be observed from Fig. 12 that mixtures prepared with Sasobit and Advera showed a higher number of cycles to failure that indicated longer service life than others. On the other hand, Rediset mix showed almost similar behaviour to original mixes. Similar N_f between the original mix and Rediset mix supports the claim that Rediset does not affect the mechanical performance of the asphalt mixture [15]. Also, having Sasobit and Advera mixes with higher N_f confirms the benefit of using WMA additives is dissipated lower energy and live longer service life.

In order to check the statistical difference between the mix types, one-way analysis of variance (ANOVA) was used in this study for each analysis method. ANOVA analysis was performed using a statistical significance level of 5% ($\alpha = 0.05$). Assuming that the null hypothesis is true, the p-value is the probability of finding a test statistic at least as extreme as the one that was truly observed. Based on the results in Table 4, since the p-value of the DPSE method is less than 0.05, the null hypothesis was rejected. Having a p-value less than 5% means that there is 95% confident level that the mean dissipated pseudo-strain energy, W_R, is statistically significant among the mixtures. However, number of cycles to failure (N_f) in the VECD analysis approach has p-value of more than 0.05 which indicated that, at 95% confident level, the mean N_f is not statistically significant among the different mixture types.

6. Conclusions

This paper aimed to study the fatigue performance of warm fine aggregate mixtures (W-FAM). An oscillatory test was performed on finger-sized samples using a Dynamic Shear Rheometer at room temperature. Experimental data were first analysed using the Superpave fatigue parameter ($G^{*}\cdot\sin\delta$). The W-FAM had a higher fatigue parameter than the control mixture. In addition, the dissipated pseudo strain energy (DPSE) of the W-FAM was less than that of the control mixture (without any WMA additive).

None of the mixtures failed up to the number of test cycles used in the test. Therefore, the viscoelastic continuum damage (VECD) approach was used in order to estimate the number of cycles to fatigue failure (N_f). There were differences in the N_f of the various mixtures; however, the analysis of variance (ANOVA) showed that there was no statistical significance in the estimated N_f among the

Table 4
Results of ANOVA of every analysis method implemented ($\alpha = 0.05$).

Analysis parameter	Mix type	Average	Variance	F value	$F_{critical}$	p-Value	Significant
DPSE, W_R at 200,000 Cycles	Original	199.27	173.09	70.773	3.098	7.9E−11	Yes
	Advera	146.66	40.19				
	Sasobit	120.65	21.40				
	Rediset	186.23	207.89				
VECD, N_f	Original	40,051	48,335,626	1.657	3.098	0.208	No
	Advera	49,930	134,928,127				
	Sasobit	49,128	388,574,205				
	Rediset	37,396	10,438,174				

F-WMA and control mixture. This finding supports that WMA has fatigue resistance that is comparable to hot mix asphalt mixtures.

Acknowledgments

This work was made possible by the NPRP award [NPRP 5-506-2-203] from the Qatar National Research Fund (a member of Qatar Foundation). The statements made herein are solely the responsibility of the authors.

References

[1] V.V. Bolotin, Mechanics of Fatigue, Mechanical, CRC Press, Minneapolis, 1999.
[2] S.A.M. Hesp, A. Soleimani, S. Subramani, T. Phillips, D. Smith, P. Marks, K.K. Tam, Asphalt pavement cracking: analysis of extraordinary life cycle variability in eastern and northeastern Ontario, Int. J. Pavement Eng. 10 (3) (2009) 209–227.
[3] S. Shen, S.H. Carpenter, Dissipated Energy Concepts for HMA Performance: Fatigue and Healing, 2007.
[4] E. Masad, V.T.F. Castelo Branco, D.N. Little, R. Lytton, An Improved Method for the Dynamic Mechanical Analysis of Fatigue Failure of Sand Asphalt Mixtures, Texas Transportation Institute, Texas A&M University (FHWA/473630), 2006.
[5] H.A.S. Sadek, Mechanistic-Based Characterisation of Fatigue Resistance of Alternative Mix Designs, University of Liverpool, 2015.
[6] J. Howson, E. Masad, A. Bhasin, System for the evaluation of moisture damage using fundamental material properties, 7(2) (2007).
[7] R. Schapery, Deformation and fracture characterization of inelastic composite materials using potentials, Polym. Eng. Sci. (7) (1987).
[8] E. Masad, V.T.F. Castelo Branco, D.N. Little, R. Lytton, A unified method for the analysis of controlled-strain and controlled-stress fatigue testing, Int. J. Pavement Eng. 9 (4) (2008) 233–246.
[9] H. Zelelew, C. Paugh, M. Corrigan, S. Belagutti, J. Ramakrishnareddy, Laboratory evaluation of the mechanical properties of plant-produced warm-mix asphalt mixtures, Road Mater. Pavement Des. 14 (1) (2013) 49–70.
[10] H. Kim, S.-J. Lee, S.N. Amirkhanian, Effects of warm mix asphalt additives on performance properties of polymer modified asphalt binders, Can. J. Civ. Eng. 37 (1) (2010) 17–24.
[11] M.M. Haggag, W.S. Mogawer, R. Bonaquist, Fatigue evaluation of warm-mix asphalt mixtures, Transp. Res. Rec. J. Transp. Res. Board 2208 (-1) (2011) 26–32.
[12] F. Safaei, J. Lee, L.A.H. Do Nascimento, C. Hintz, Y.R. Kim, Implications of warm-mix asphalt on long-term oxidative ageing and fatigue performance of asphalt binders and mixtures, Road Mater. Pavement Des. 15 (sup1) (2014) 45–61.
[13] Sasol Wax, Sasobit – Sasolwax US, 2014. [Online]. Available: <http://www.sasolwax.us.com/>.
[14] PQ Corporation, Advera Warm mix asphalt, 2014. [Online]. Available: <http://www.adverawma.com/wma.html>.
[15] AkzoNobel, Rediset LQ - AkzoNobel Asphalt Applications, 2014. [Online]. Available: <http://sc.akzonobel.com/en/asphalt/Pages/new-product-rediset-LQ.aspx>.
[16] V.T.F. Castelo Branco, E. Masad, A. Bhasin, D.N. Little, Fatigue analysis of asphalt mixtures independent of mode of loading, Transp. Res. Rec. J. Transp. Res. Board 2057 (-1) (2008) 149–156.
[17] C. Branco, V. Franco, V.T.F.C. Branco, A Unified Method for the Analysis of Nonlinear Viscoelasticity and Fatigue Cracking of Asphalt Mixtures using the Dynamic Mechanical Analyzer, Texas A&M University, 2008.
[18] A.E. Martin, E. Arambula, F. Yin, L.G. Cucalon, A. Chowdhury, R. Lytton, J. Epps, C. Estakhri, E.S. Park, Evaluation of the Moisture Susceptibility of WMA Technologies, 2014 (College Station, TX).
[19] W. Herb, M. Marasteanu, H.G. Stefan, Simulation and Characterization of Asphalt Pavement Temperatures, 2006.
[20] J. D'Angelo, R. Kluttz, R. Dongre, K. Stephens, Revision of the superpave high temperature binder specification: the multiple stress creep recovery test (with discussion), J. Assoc. Asphalt Paving Technol. 76 (2007) 123–162.
[21] R.A. Schapery, Nonlinear fracture analysis of viscoelastic composite materials based on a generalized J integral theory, in: Proceedings Japan-U.S, 1981.
[22] E. Kutay, N. Gibson, J. Youtcheff, Conventional and viscoelastic continuum damage (VECD)-based fatigue analysis of polymer modified asphalt pavements, Asphalt Paving Technol. 77 (2008) 395–433.
[23] E. Kutay, H. Gibson, J. Youtcheff, Use of pseudostress and pseudostrain concepts for characterization of asphalt fatigue tests, Mech. Model. Detect. Test. Case Hist. Kutay 5 (019) (2008) 305–314.
[24] Y. Kim, D. Little, R. Lytton, Use of dynamic mechanical analysis (DMA) to evaluate the fatigue and healing potential of asphalt binders in sand asphalt mixtures, Asphalt Paving Technol. 71 (2002) 176–206.
[25] A. Bhasin, V.T. Castelo Branco, E. Masad, D.N. Little, Quantitative comparison of energy methods to characterize fatigue in asphalt materials, J. Mater. Civ. Eng. 21 (2) (2009) 83–92.
[26] Y. Kim, I. Song, D. Little, Use of dynamic mechanical analysis to predict damage in asphalt mastic, in: Proc. 11th Annu. Int. Cent. . . ., 2003.
[27] E. Masad, C. Huang, J. D'Angelo, D. Little, Characterization of asphalt binder resistance to permanent deformation based on nonlinear viscoelastic analysis of multiple stress creep recovery (MSCR) test, in: Asphalt Paving Technology 2009, AAPT, 2009, pp. 535–562.
[28] H. Sadek, H. Al-Khalid, E. Masad, O. Sirin, H. Khaled, Characterisation of fatigue resistance of alternative pavement design for the state of Qatar, in: Sustainability, Eco-Efficiency and Conservation in Transportation Infrastructure Asset Management, 2014, pp. 433–439.
[29] B. Underwood, Multiscale Constitutive Modeling of Asphalt Concrete, 2011.
[30] H. Lee, Y. Kim, Viscoelastic continuum damage model of asphalt concrete with healing, J. Eng. Mech. (1998) 1224–1232 (no. Schapery 1990).
[31] E. Kutay, N. Gibson, J. Youtcheff, R. Dongré, Use of small samples to predict fatigue lives of field cores, Transp. Res. Rec. J. Transp. Res. Board 2127 (Dec. 2009) 90–97.
[32] C. Zollinger, Application of Surface Energy Measurements to Evaluate Moisture Susceptibility of Asphalt and Aggregates, Texas A&M University, 2005.
[33] K.A. Ghuzlan, S.H. Carpenter, Energy-derived, damage-based failure criterion for fatigue testing, Transp. Res. Rec. 1723 (2000) 141–149.
[34] B.S. Underwood, C. Baek, Y.R. Kim, Simplified viscoelastic continuum damage model as platform for asphalt concrete fatigue analysis, Transp. Res. Rec. J. Transp. Res. Board 2296 (-1) (2012) 36–45.